

Muon Decay

W. Fetscher^{1*}

¹ Institute for Physics and Astrophysics, ETH Zürich

* fetscher@phys.ethz.ch

July 6, 2021



Review of Particle Physics at PSI
doi:[10.21468/SciPostPhysProc.2](https://doi.org/10.21468/SciPostPhysProc.2)

Abstract

The decay of the muon has been studied at PSI with several precision measurements: The longitudinal polarization $P_L(E)$ with the muon decay parameters ξ' , ξ'' , the Time-Reversal Invariance (TRI) conserving transverse polarization $P_{T_1}(E)$ with the muon decay parameters η , η'' , the TRI violating transverse polarization $P_{T_2}(E)$, with α'/A , β'/A and the muon decay asymmetry with $P_\mu\xi$. The detailed theoretical analysis of all measurements of normal and inverse muon decay has led for the first time to a lower limit $|g_{LL}^V| > 0.960$ ("V-A") and upper limits for nine other possible complex couplings, especially the scalar coupling $|g_{LL}^S| < 0.550$ which had not been excluded before.

6.1 Introduction

Muon decay, $\mu^+ \rightarrow \bar{\nu}_\mu e^+ \nu_e$, as a purely leptonic process, provides a precise source of information on the charged current weak interaction. Before the advent of the meson factories LAMPF, TRIUMF and SIN, experimental results were scarce and theoretical descriptions inappropriate to uniquely deduce the interaction. In a combined effort, the ETH-SIN group has performed decisive precision measurements and, simultaneously, developed the theoretical description in a way that allowed the determination of the interaction from experimental results, taken exclusively from normal and inverse muon decay ($\nu_\mu + e^- \rightarrow \mu^- + \nu_e$).

6.2 General Matrix Element

The three leptonic decays $\mu^+ \rightarrow \bar{\nu}_\mu e^+ \nu_e$, $\tau^+ \rightarrow \bar{\nu}_\tau \mu^+ \nu_\mu$ and $\tau^+ \rightarrow \bar{\nu}_\tau e^+ \nu_e$, as well as their charge conjugate decays, can be described by the most general, local, derivative-free and lepton-number conserving four-fermion contact interaction Hamiltonian. The contact interaction allows the use of equivalent Hamiltonians, which differ in the way the fermions are grouped together [1, 2]. The older literature preferred a "charge retention" form with parity-odd and parity-even terms in which e^+ and μ^+ , as the usually detected particles, were grouped together [3, 4]. This had the advantage that limits to some coupling constants could be obtained from then existing results. The disadvantage was that this Hamiltonian represents interactions proceeding via the exchange of a neutral boson X that would carry the lepton numbers both of muon and electron, and so would not be universal. The use of a "charge-changing" form, where the charged leptons are grouped with their neutrinos and which is adapted to charged boson exchange, results in absolute values of differences of coupling constants. Both of these forms are complicated by the fact that a fully parity-violating interaction, such as e.g. the $V-A$ interaction, is represented by four coupling constants C_V , C'_V , C_A and C'_A .

39 In the following, we will use a charge-changing Hamiltonian characterized by fields of
 40 definite chirality [5, 6]. We use the notation of Fetscher *et. al.* [7], which in turn uses the sign
 41 conventions and definitions of Scheck [8]. The general matrix element can then be written as

$$M = 4 \frac{G_F}{\sqrt{2}} \sum_{\substack{\gamma=S,V,T \\ \varepsilon,\mu=R,L}} g_{\varepsilon\mu}^\gamma \langle \bar{e}_\varepsilon | \Gamma^\gamma | (\nu_e)_n \rangle \langle (\bar{\nu}_\mu)_m | \Gamma_\gamma | \mu_\mu \rangle. \quad (6.1)$$

42 Here, G_F is the Fermi coupling constant, while $\gamma = S, V, T$ indicates a 4-scalar, 4-vector, or
 43 4-tensor interaction; the corresponding Γ^γ could be either Dirac γ matrices or, when using the
 44 Weyl spinors of Eqs. (6.2) to (6.4), Pauli matrices. The indices $\varepsilon, \mu = R, L$ indicate the chirality
 45 (right- or left-handed) of the spinors of the electron or muon. The chiralities n and m of the
 46 ν_e and $\bar{\nu}_\mu$ are then determined by the values of γ, ε , and μ . In this picture, the coupling con-
 47 stants $g_{\varepsilon\mu}^\gamma$ have a simple physical interpretation: $n_\gamma |g_{\varepsilon\mu}^\gamma|^2$ is equal to the (relative) probability
 48 for a μ -handed muon to decay into an ε -handed electron by the interaction Γ^γ ; the factors
 49 $n_S = 1/4$, $n_V = 1$ and $n_T = 3$ take care of the proper normalisation. The standard model thus
 50 corresponds to $g_{LL}^V = 1$, with all other couplings being zero.

51 We emphasise that here right- and left-handed definitely means chirality and not helicity.
 52 The left-handed spinor $\overset{\circ}{\chi}$ of a fermion in its rest system transforms under a Lorentz-boost as

$$\chi_L(\mathbf{p}) = \frac{(E+m)\sigma^0 - \mathbf{p} \cdot \boldsymbol{\sigma}}{\sqrt{2m(E+m)}} \overset{\circ}{\chi}, \quad (6.2)$$

53 where σ^0 and $\boldsymbol{\sigma}$ are the four Pauli matrices. By a parity operation, $\chi_L(\mathbf{p})$ becomes the right-
 54 handed spinor $\chi_R(\mathbf{p})$. Left- and right-handed spinors are contained in separate $\mathbb{C}2$ -spaces.
 55 The right-handed spinor transforms under a Lorentz-boost as

$$\chi_R(\mathbf{p}) = \frac{(E+m)\sigma^0 + \mathbf{p} \cdot \boldsymbol{\sigma}}{\sqrt{2m(E+m)}} \overset{\circ}{\chi}. \quad (6.3)$$

56 The spinor of the antiparticle is given by

$$\varphi_L(\mathbf{p}) = +i\sigma^2 \chi_R^*(\mathbf{p}) \quad \text{and} \quad \varphi_R(\mathbf{p}) = -i\sigma^2 \chi_L^*(\mathbf{p}). \quad (6.4)$$

57 6.3 Observables

58 The differential decay probability to obtain an e^\pm with (reduced) energy between x and $x+dx$,
 59 emitted in the direction \hat{x}_3 at an angle between ϑ and $\vartheta+d\vartheta$ with respect to the muon polar-
 60 ization vector \mathbf{P}_μ , and with its spin parallel to the arbitrary direction $\hat{\zeta}$, neglecting radiative
 61 corrections, is given by

$$\frac{d^2\Gamma}{dx d\cos\vartheta} = \frac{m_\mu}{4\pi^3} W_{e\mu}^4 G_F^2 \sqrt{x^2 - x_0^2} \cdot \{F_{IS}(x) \pm P_\mu \cos\vartheta F_{AS}(x)\} \cdot \{1 + \hat{\zeta} \cdot \mathbf{P}_e(x, \vartheta)\}. \quad (6.5)$$

62 Here, $W_{e\mu} = \max(E_e) = (m_\mu^2 + m_e^2)/(2m_\mu)$ is the maximum e^\pm energy, $x = E_e/W_{e\mu}$ is the re-
 63 duced energy, $x_0 = m_e/W_{e\mu} = 9.67 \times 10^{-3}$, and $P_\mu = |\mathbf{P}_\mu|$ is the degree of muon polarization.
 64 $\hat{\zeta}$ is the direction in which a perfect polarization-sensitive electron detector is most sensitive.
 65 The isotropic part of the spectrum, $F_{IS}(x)$, the anisotropic part $F_{AS}(x)$, and the electron po-
 66 larization, $\mathbf{P}_e(x, \vartheta)$, may be parameterized by the Michel parameter ρ [1], by η [9], by ξ and
 67 δ [3, 10], *etc.* These are bilinear combinations of the coupling constants $g_{\varepsilon\mu}^\gamma$, which occur in
 68 the matrix element (given below).

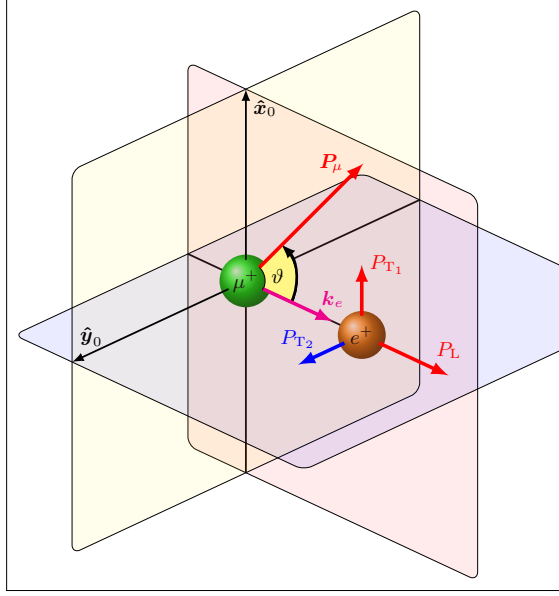


Figure 6.1: Definition of the observables in polarized muon decay: muon polarization \mathbf{P}_μ , positron momentum \mathbf{k}_e , longitudinal positron polarization P_L , transverse positron polarization (P_{T_1} , P_{T_2}) and angle of emission ϑ (relative to \mathbf{P}_μ). Time reversal invariance is violated if $P_{T_2} \neq 0$. From [11].

69 If the masses of the neutrinos as well as x_0 are neglected, the energy and angular distri-
 70 bution of the electron in the rest frame of a muon (μ^\pm) measured by a polarization insensitive
 71 detector is given by

$$\frac{d^2\Gamma}{dx d\cos\vartheta} \sim x^2 \cdot \left\{ 3(1-x) + \frac{2\rho}{3}(4x-3) + 3\eta x_0(1-x)/x \right. \\ \left. \pm P_\mu \cdot \xi \cdot \cos\vartheta \left[1-x + \frac{2\delta}{3}(4x-3) \right] \right\}. \quad (6.6)$$

72 Here, ϑ is the angle between the electron momentum and the muon spin, and $x \equiv 2E_e/m_\mu$.
 73 Within the Standard Model, we obtain $\rho = \xi\delta = 3/4$, $\xi = 1$, $\eta = 0$ and the differential decay
 74 rate is

$$\frac{d^2\Gamma}{dx d\cos\vartheta} = \frac{G_F^2 m_\mu^5}{192\pi^3} [3 - 2x \pm P_\mu \cos\vartheta(2x-1)] x^2. \quad (6.7)$$

75 The coefficient in front of the square bracket is the total decay rate.

76 The observables in the decay of polarized muons are shown in Figure 6.1. We have defined
 77 a right-handed coordinate system with

$$\hat{\mathbf{z}}_0 = \frac{\mathbf{k}_e}{|\mathbf{k}_e|}, \quad \hat{\mathbf{y}}_0 = \frac{\mathbf{k}_e \times \mathbf{P}_\mu}{|\mathbf{k}_e \times \mathbf{P}_\mu|}, \quad \hat{\mathbf{x}}_0 = \hat{\mathbf{y}}_0 \times \hat{\mathbf{z}}_0. \quad (6.8)$$

78 Here, \mathbf{k}_e is the momentum vector of the electron, while P_L designates the longitudinal po-
 79 larization, P_{T_1} the transverse component of \mathbf{P}_e lying in the plane defined by \mathbf{k}_e and \mathbf{P}_μ , and
 80 P_{T_2} is the component perpendicular to that plane. $P_{T_2} \neq 0$ signals violation of time-reversal

81 symmetry. These polarization components are

$$P_{T_1}(x, \vartheta) = \frac{P_\mu \sin \vartheta \cdot F_{T_1}(x)}{F_{IS}(x) \pm P_\mu \cos \vartheta \cdot F_{AS}(x)}, \quad (6.9)$$

$$P_{T_2}(x, \vartheta) = \frac{P_\mu \sin \vartheta \cdot F_{T_2}(x)}{F_{IS}(x) \pm P_\mu \cos \vartheta \cdot F_{AS}(x)}, \quad (6.10)$$

$$P_L(x, \vartheta) = \frac{\pm F_{IP}(x) + P_\mu \cos \vartheta \cdot F_{AP}(x)}{F_{IS}(x) \pm P_\mu \cos \vartheta \cdot F_{AS}(x)}. \quad (6.11)$$

82 If only the neutrino masses are neglected, and if the e^\pm polarization is detected, then the
83 functions in (6.5) can be decomposed as [12]

$$F_\nu(x) = F_\nu^{V-A}(x) + G_\nu(x), \quad (6.12)$$

84 where $G_\nu(x) \equiv 0$ for $g_{LL}^V = 1$ ("V - A"). Physics beyond the Standard Model would thus be
85 contained *exclusively* in the $G_\nu(x)$. The index ν stands for IS (isotropic part of the spectrum),
86 AS (anisotropic part of the spectrum), T_1 (transverse polarization P_{T_1}), T_2 (transverse polar-
87 ization P_{T_2}), IP (isotropic part of the longitudinal polarization) and AP (anisotropic part of the
88 longitudinal polarization). The $F_\nu^{V-A}(x)$ do not depend on specific decay parameters:

$$F_{IS}^{V-A}(x) = \frac{1}{6} \{-2x^2 + 3x - x_0^2\}, \quad (6.13a)$$

$$F_{AS}^{V-A}(x) = \frac{1}{6} (x^2 - x_0^2)^{1/2} \{2x - 2 + (1 - x_0^2)^{1/2}\}, \quad (6.13b)$$

$$F_{T_1}^{V-A}(x) = -\frac{1}{6} / (1 - x) x_0, \quad (6.13c)$$

$$F_{T_2}^{V-A}(x) = 0, \quad (6.13d)$$

$$F_{IP}^{V-A}(x) = \frac{1}{6} (x^2 - x_0^2)^{1/2} \{-2x + 2 + (1 - x_0^2)^{1/2}\}, \quad (6.13e)$$

$$F_{AP}^{V-A}(x) = \frac{1}{6} \{-2x^2 - x - x_0^2\}. \quad (6.13f)$$

89 The functions $G_\nu(x)$ depend on the decay parameters $\rho, \xi'', \xi', \xi, \delta, \eta, \eta'', \alpha'/A, \beta'/A$, where
90 $\eta = (\alpha - 2\beta)/A$ and $\eta'' = (3\alpha + 2\beta)/A$:

$$G_{IS}(x) = \frac{1}{9} \{2(\rho - \frac{3}{4})(4x^2 - 3x - x_0^2) + 9\eta(1 - x)x_0\}, \quad (6.14a)$$

$$G_{AS}(x) = \frac{1}{9} (x^2 - x_0^2)^{1/2} \{3(\xi - 1)(1 - x), \\ + 2(\xi\delta - \frac{3}{4})(4x - 4 + (1 - x_0^2)^{1/2})\}, \quad (6.14b)$$

$$G_{T_1}(x) = \frac{1}{12} \left\{ -2 \left[(\xi'' - 1) + 12 \left(\rho - \frac{3}{4} \right) \right] (1 - x) x_0 \right. \\ \left. - 3\eta (x^2 - x_0^2) + \eta'' (-3x^2 + 4x - x_0^2) \right\}, \quad (6.14c)$$

$$G_{T_2}(x) = \frac{1}{3} (x^2 - x_0^2)^{1/2} \left\{ 3 \frac{\alpha'}{A} (1 - x) + 2 \frac{\beta'}{A} (1 - x_0^2)^{1/2} \right\}, \quad (6.14d)$$

$$G_{IP}(x) = \frac{1}{54} (x^2 - x_0^2)^{1/2} \left\{ 9(\xi' - 1) \left[-2x + 2 + (1 - x_0^2)^{1/2} \right] \right. \\ \left. + 4\xi \left(\delta - \frac{3}{4} \right) \left[4x - 4 + (1 - x_0^2)^{1/2} \right] \right\}, \quad (6.14e)$$

$$G_{AP}(x) = \frac{1}{6} \{ (\xi'' - 1) (2a^2 - x - x_0^2) + 4(\rho - \frac{3}{4})(4x^2 - 3x - x_0^2) \\ + 2\eta''(1 - x)x_0 \}. \quad (6.14f)$$

91 Several of the decay parameters $\{\rho, \xi, \xi', \xi'', \delta, \eta, \eta'', \alpha/A, \beta/A, \alpha'/A, \beta'/A\}$, which are not
92 all independent, have been measured in the past. Past experiments have also been analyzed

93 using the parameters $a, b, c, a', b', c', \alpha/A, \beta/A, \alpha'/A, \beta'/A$ (and $\eta = (\alpha - 2\beta)/2A$), as defined
 94 by Kinoshita and Sirlin [3, 10]. They serve as a model-independent summary of all possible
 95 measurements on the decay electron (see Listings below). The relations between the two sets
 96 of parameters are

$$\rho - \frac{3}{4} = \frac{3}{4}(-a + 2c)/A, \quad (6.15)$$

$$\eta = (\alpha - 2\beta)/A, \quad (6.16)$$

$$\eta'' = (3\alpha + 2\beta)/A, \quad (6.17)$$

$$\delta - \frac{3}{4} = \frac{9}{4} \frac{(a' - 2c')/A}{1 - [a + 3a' + 4(b + b') + 6c - 14c']/A}, \quad (6.18)$$

$$1 - \xi \frac{\delta}{\rho} = 4 \frac{[(b + b') + 2(c - c')]/A}{1 - (a - 2c)/A}, \quad (6.19)$$

$$1 - \xi' = [(a + a') + 4(b + b') + 6(c + c')]/A, \quad (6.20)$$

$$1 - \xi'' = (-2a + 20c)/A, \quad (6.21)$$

97 where

$$A = a + 4b + 6c. \quad (6.22)$$

98 The ten complex amplitudes $g_{\varepsilon\mu}^\gamma$ (g_{RR}^T and g_{LL}^T are identically zero) and G_F constitute 20 inde-
 99 pendent (real) parameters to be determined by experiment. The Standard Model interaction
 100 corresponds to one single amplitude g_{LL}^V being unity and all the others being zero.

101 6.4 Lorentz Structure

102 The nine parameters $\{\rho, \xi, \xi', \xi'', \delta, \eta, \eta'', \alpha'/A, \beta'/A\}$ describing the electron spectrum,
 103 decay asymmetry and polarization vector can be represented [3] by the intermediate quantities
 104 $\{a, a', \alpha, \alpha', b, b', \beta, \beta', c, c'\}$, whose values are known from experiment [13]. They are all
 105 real, bilinear combinations of the coupling constants:

$$a = 16(|g_{RL}^V|^2 + |g_{LR}^V|^2) + |g_{RL}^S + 6g_{RL}^T|^2 + |g_{LR}^S + 6g_{LR}^T|^2, \quad (6.23a)$$

$$a' = 16(|g_{RL}^V|^2 - |g_{LR}^V|^2) + |g_{RL}^S + 6g_{RL}^T|^2 - |g_{LR}^S + 6g_{LR}^T|^2, \quad (6.23b)$$

$$\alpha = 8\text{Re}\{g_{LR}^V(g_{RL}^{S*} + 6g_{RL}^{T*}) + g_{RL}^V(g_{LR}^{S*} + 6g_{LR}^{T*})\}, \quad (6.23c)$$

$$\alpha' = 8\text{Im}\{g_{LR}^V(g_{RL}^{S*} + 6g_{RL}^{T*}) - g_{RL}^V(g_{LR}^{S*} + 6g_{LR}^{T*})\}, \quad (6.23d)$$

$$b = 4(|g_{RR}^V|^2 + |g_{LL}^V|^2) + |g_{RR}^S|^2 + |g_{LL}^S|^2, \quad (6.23e)$$

$$b' = 4(|g_{RR}^V|^2 - |g_{LL}^V|^2) + |g_{RR}^S|^2 - |g_{LL}^S|^2, \quad (6.23f)$$

$$\beta = -4\text{Re}\{g_{RR}^V g_{LL}^{S*} + g_{LL}^V g_{RR}^{S*}\}, \quad (6.23g)$$

$$\beta' = 4\text{Im}\{g_{RR}^V g_{LL}^{S*} - g_{LL}^V g_{RR}^{S*}\}, \quad (6.23h)$$

$$c = \frac{1}{2}\{|g_{RL}^S - 2g_{RL}^T|^2 + |g_{LR}^S - 2g_{LR}^T|^2\}, \quad (6.23i)$$

$$c' = \frac{1}{2}\{|g_{RL}^S - 2g_{RL}^T|^2 - |g_{LR}^S - 2g_{LR}^T|^2\}. \quad (6.23j)$$

106 From (6.23a) to (6.23j) it can be seen that these quantities are not completely independent.
 107 The transformation from the 20-dimensional space of the complex $g_{\varepsilon\mu}^\gamma$ to the 10-dimensional
 108 space of the $\{a, \dots, c'\}$ leads to the following constraints [14]:

$$a \geq 0 \quad a^2 \geq a'^2 + \alpha^2 + \alpha'^2, \quad (6.24)$$

$$b \geq 0 \quad b^2 \geq b'^2 + \beta^2 + \beta'^2, \quad (6.25)$$

$$c \geq 0 \quad c^2 \geq c'^2. \quad (6.26)$$

109 These constraints are very important for any general analysis of muon decay, as they strongly
 110 influence the final errors of the quantities they relate.

111 The precise measurement of individual decay parameters alone generally does not give
 112 conclusive information about the kind of interaction due to the many different couplings and
 113 the interference terms between them. A good example for this is the famous Michel parameter
 114 ϱ . A precise measurement yielding the value $3/4$ as predicted by $V-A$ by no means establishes
 115 the $V-A$ interaction. In fact any interaction consisting of an arbitrary combination of g_{LL}^S ,
 116 g_{LR}^S , g_{RL}^S , g_{RR}^S , g_{LR}^V and g_{LL}^V will yield exactly $\varrho = \frac{3}{4}$. This can be seen if we write ϱ in the
 117 form [15]

$$\varrho - \frac{3}{4} = -\frac{3}{4} \{ |g_{LR}^V|^2 + |g_{RL}^V|^2 + 2(|g_{LR}^T|^2 + |g_{RL}^T|^2) - \text{Re}(g_{LR}^S g_{LR}^{T*} + g_{RL}^S g_{RL}^{T*}) \}. \quad (6.27)$$

118 For $\varrho = 3/4$ and $g_{LR}^T = g_{RL}^T = 0$ (no tensor interaction) we find $g_{LR}^V = g_{RL}^V = 0$, with all the
 119 remaining six couplings being arbitrary!

120 The magnitude of the interaction is contained in the Fermi coupling constant G_F . Thus the
 121 $g_{\mu\nu}^\gamma$ may be normalized, dimensionless coupling constants, resulting in

$$A \equiv a + 4b + 6c = 16. \quad (6.28)$$

122 This is equivalent to

$$Q_{RR} + Q_{LR} + Q_{RL} + Q_{LL} = 1, \quad (6.29)$$

123 where

$$Q_{RR} = \frac{1}{4} |g_{RR}^S|^2 + |g_{RR}^V|^2, \quad (6.30)$$

$$Q_{RL} = \frac{1}{4} |g_{RL}^S|^2 + |g_{RL}^V|^2 + 3|g_{RL}^T|^2, \quad (6.31)$$

$$Q_{LR} = \frac{1}{4} |g_{LR}^S|^2 + |g_{LR}^V|^2 + 3|g_{LR}^T|^2, \quad (6.32)$$

$$Q_{LL} = \frac{1}{4} |g_{LL}^S|^2 + |g_{LL}^V|^2. \quad (6.33)$$

124 We note that $0 \leq Q_{\varepsilon\mu} \leq 1$ and $\sum_{\varepsilon\mu} Q_{\varepsilon\mu} = 1$. $Q_{\varepsilon\mu}$ is then the probability for the decay of a
 125 muon of handedness μ into an electron of handedness ε . The main point is now that the $Q_{\varepsilon\mu}$
 126 can be expressed by the known quantities $\{a, \dots, c'\}$ [7]:

$$Q_{RR} = 2(b + b')/A, \quad (6.34)$$

$$Q_{RL} = [(a - a') + 6(c - c')]/(2A), \quad (6.35)$$

$$Q_{LR} = [(a + a') + 6(c + c')]/(2A), \quad (6.36)$$

$$Q_{LL} = 2(b - b')/A. \quad (6.37)$$

127 In the Standard Model, $Q_{LL} = 1$ while the others are zero. The existing measurements show
 128 that the three probabilities Q_{RR} , Q_{LR} and Q_{LL} are zero, within errors. This gives upper limits to
 129 the absolute values of eight of the ten complex coupling constants. Furthermore, we find that
 130 Q_{LL} is bounded by a lower limit which shows that both muon and electron are left-handed.
 131 It can be seen from (6.33), however, that the data from the measurements of the muon and
 132 the electron observables do not allow one to distinguish a vector (g_{LL}^V) from a scalar (g_{LL}^S)
 133 interaction. This type of ambiguity has been noted before in the context of a different Hamil-
 134 tonian [16, 17] and electron-neutrino correlation measurements (not performed up to date)
 135 have been proposed. The total rate S , normalized to the rate predicted by $V-A$ for the reac-
 136 tion $\nu_\mu + e^- \rightarrow \mu^- + \nu_e$ with ν_μ of negative helicity, has been found to be close to 1 [17, 18].
 137 S effectively depends only on those five coupling constants g_{LL}^V , g_{RL}^V , g_{LR}^S , g_{LR}^T and g_{RR}^S that

138 describe interactions with a left-handed ν_μ . The four latter coupling constants are found to be
 139 small. One thus obtains [7]

$$S = |g_{LL}^V|^2. \quad (6.38)$$

140 which yields a *lower* limit for $|g_{LL}^V|$, and through the normalisation requirement (6.29) an
 141 upper limit for the remaining $|g_{LL}^S|$:

$$|g_{LL}^S| < 2\sqrt{1-S}. \quad (6.39)$$

142 Thus the weak interaction has been completely determined for muon decay using only data
 143 from this purely leptonic interaction.

144 6.5 Experiments

145 6.5.1 Longitudinal Positron Polarization

146 The measurement of the longitudinal polarization P_L of the electrons from the decay of polar-
 147 ized or unpolarized muons allows the determination of the parameters ξ' and ξ'' , as can be
 148 seen from Eqs. (6.11), (6.12), (6.14e) and (6.14f). The parameter ξ' is of special interest. In
 149 terms of the coupling constants $g_{\varepsilon\mu}^\gamma$ we have

$$\begin{aligned} 1 - \xi' &= \frac{1}{2} \{ 4 \cdot (|g_{RR}^V|^2 + |g_{RL}^V|^2) + (|g_{RR}^S|^2 + |g_{RL}^S|^2) + 12 \cdot |g_{RL}^T|^2 \} \\ &= 2(Q_{RR} + Q_{RL}) \equiv 2Q_R^e, \end{aligned} \quad (6.40)$$

150 where Q_R^e is the probability of the decay of a muon with chirality μ into an electron with
 151 chirality ε . Note that (6.40) is a sum of absolute squares where only coupling constants with
 152 $\varepsilon = R$ appear. A deviation of ξ' from 1 would require the existence of a coupling with the right-
 153 handed components of the electron, i.e. at least one $g_{R\mu}^\gamma \neq 0$. Conversely, a measurement with
 154 the result $\xi' = 1$ would prove that the coupling acts exclusively on the left-handed component
 155 of the electron.

156 To determine ξ' , the longitudinal polarization P_L of the electrons from unpolarized muons
 157 has been measured. For the purpose of illustration, we neglect the electron mass m_e and use
 158 the experimentally well confirmed values $\varrho = \delta = \frac{3}{4}$ and obtain from (6.11)

$$\xi' = P_L. \quad (6.41)$$

159 The measurement of the electron's longitudinal polarization P_L consists of a comparison with
 160 the spin polarization of the electrons contained in a piece of saturated ferromagnetic material
 161 [19–21]. The comparison is done by scattering the decay electrons from the electrons of a
 162 ferromagnet, using the fact that relativistic electron-electron scattering most often occurs when
 163 the two spins have opposite directions.

164 The experiment was performed at the $\pi E1$ beam line at SIN. A schematic view of the appa-
 165 ratus is shown in Figure 6.2. The 150-MeV/c π^+ beam was stopped in an oak target, where the
 166 π^+ decay resulted in an unpolarized sample of μ^+ within the oak target. Positrons from muon
 167 decay crossed a magnetised iron foil, where they could annihilate in flight with polarized elec-
 168 trons (ANN), $e^+e^- \rightarrow \gamma\gamma$, or scatter elastically: Bhabha-scattering (BHA), $e^+e^- \rightarrow e^+e^-$. Both
 169 reactions have high analysing powers up to 90%. The electron polarization in the iron foil
 170 was $(54.44 \pm 0.56) \times 10^{-3}$. The final result of this experiment is [14]

$$\langle |P_L| \rangle = 0.998 \pm 0.042. \quad (6.42)$$

171 From the resulting error of ξ' , which is dominated by the error of $\langle |P_L| \rangle$, upper limits for all
 172 couplings of right-handed electrons to muons (of any handedness) $g_{R\mu}^\gamma, \mu = R, L$, follow, in

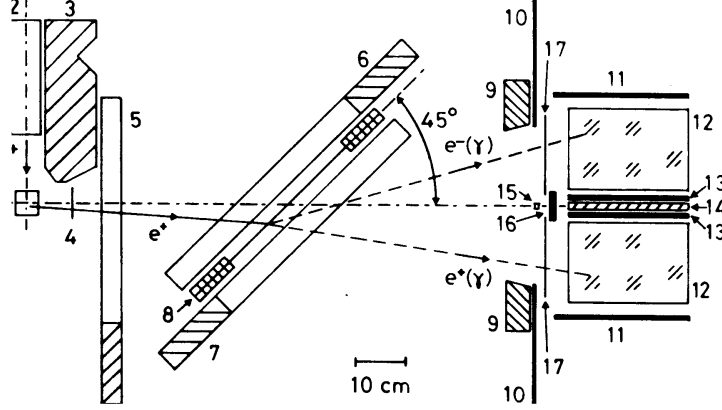


Figure 6.2: Schematic top view of the apparatus used for the measurement of P_L . A typical event is shown for either ANN or BHA. The experimental arrangement: (1) oak stopping target; (2) Be-CH₂ moderator; (3) shielding; (4) timing counter; (5), (6), and (7) multiwire proportional chambers labeled in the text WC₁, WC₂, and WC₃, respectively; and (8) magnet with iron foil. The total-absorption spectrometer is symmetric to the central axis. It consists of (12) four NaI detectors (only the upper pair is shown); (9) square Pb collimator; (10) square-aperture anticoincidence counter; (15) Am-Be calibration source; (17) four electron-identification counters; (16) vertical anticoincidence counter and monitor; (11) and (13) vertical anticoincidence counters; (14) vertical Fe-Pb photon converters. Not shown are the horizontal counterparts of (11), (13), (14) and (16).

173 principle, from (6.40). Improved values of these limits are obtained for $|g_{RL}^V|$ and $|g_{RL}^S + 6g_{RL}^T|$
 174 by also considering

$$B_{RL} = \frac{1}{16}|g_{RL}^S + 6g_{RL}^T|^2 + |g_{RL}^V|^2 = \frac{1}{2A}(a + a'). \quad (6.43)$$

175 The parameter ξ'' in μ^+ decay has been determined from a measurement of $P_L(x, \vartheta)$ as
 176 a function of the reduced energy x and the angle ϑ between the muon spin and the positron
 177 momentum [14]. The precision of the measured combination $(\xi'' - \xi\xi')/\xi = -0.35 \pm 0.33$
 178 does, however, not lead to better constraints of the couplings. With a new dedicated setup this
 179 value was considerably improved to [22]

$$\xi'' = 0.981 \pm 0.045_{\text{stat.}} \pm 0.003_{\text{syst.}}. \quad (6.44)$$

180 6.5.2 Transverse Positron Polarization

181 The transverse electron polarization $\mathbf{P}_T = (P_{T_1}, P_{T_2})$ is defined in Figure 6.1 and Eqs. (6.9)
 182 and (6.10). Independent of any assumption about the mechanism of muon decay or even
 183 the nature of the two unobserved neutral particles, time reversal invariance (disregarding the
 184 negligible final state interactions) requires $P_{T_2} = 0$.

185 The measurement of \mathbf{P}_T as a function of energy yields a determination of the parameters
 186 η , η'' , α/A and α'/A (see Eqs. (6.16), (6.17), (6.23d) and (6.23h)). η is of special interest. η ,
 187 together with the Michel parameter ρ , determines the shape of the (isotropic) positron energy
 188 spectrum. However, it is difficult to deduce its value from a spectrum measurement, as its
 189 influence is suppressed by a factor $x_0 \approx 10^{-2}$. On the other hand, a precise value is needed

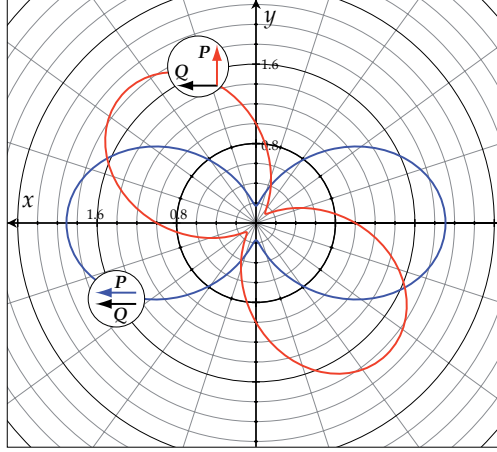


Figure 6.3: Intensity distributions of the annihilation photons at $E_3 = E_4 = 50 m_e$ for parallel spins ($e^- : Q = 1, e^+ : P_T = 1$) and for perpendicular spins. The maximum of the intensity lies on the bisector of the angle ωt between the two spins. Thus the “figure of eight” moves with angular frequency $\omega/2$. For a fixed detector pair at azimuthal angle ψ the time dependence is still given by the angular frequency ω due to the two symmetric lobes of the “figure of eight”. From [11, 24].

190 for a precise determination of ϱ , as η and ϱ are statistically highly correlated. In (6.14c) for
 191 P_{T_1} , η arises without a suppression factor. It is interesting to note that P_{T_1} does not vanish in
 192 the Standard Model interaction, as can be seen from (6.9), and it may take sizeable values
 193 ($|P_{T_1}| \leq 1/3$) for positron energies of a few MeV.

194 The experiment was performed with basically the same setup used for measuring the longi-
 195 tudinal polarization. It also uses a comparison with the spin polarized electrons in a ferromag-
 196 netic foil from annihilation in flight $e^+e^- \rightarrow \gamma\gamma$. It is based on the fact that the photons from
 197 the annihilation of a relativistic, transversely polarized positron electron pair are preferentially
 198 emitted in the plane defined by the particle line-of-flight \mathbf{k}_{e^+} and the bisector \mathbf{b} between the
 199 (transverse) polarization directions \mathbf{p}_T and \mathbf{p}_{e^-} (see Figure 6.3).

200 The results of a general, unrestricted analysis of the data are an improved value for
 201 $\eta = (11 \pm 85) \times 10^{-3}$ and the first results for $\eta'' = (48 \pm 125) \times 10^{-3}$ and the T-violating
 202 parameters $\alpha' = (-47 \pm 52) \times 10^{-3}$ and $\beta' = (17 \pm 18) \times 10^{-3}$ [13].

203 An improved experiment, where all the major parts of the previous experiment have been
 204 replaced by newly designed equipment to increase the event rate and reduce the systematic
 205 errors, has been described in detail elsewhere [25]. The four NaI detectors were replaced by an
 206 array of 127 BGO detectors (see Figure 6.4). A longitudinally polarized μ^+ beam ($P_\mu^b = 91\%$)
 207 enters a beryllium stop target with bunches every 19.75 ns. The polarization $P_\mu(t)$ of the
 208 stopped muons precesses in a homogeneous magnetic field ($B = 373.6 \pm 0.4$ mT) with the
 209 same angular frequency ω as the accelerator radio frequency. This ensures that $P_\mu(t) \parallel P_\mu^b$ for
 210 each newly arriving μ^+ bunch. Because of the burst width of 3.9 ns (FWHM) the polarization
 211 $P_\mu(0)$ of the stopped μ^+ is reduced to $(82 \pm 2)\%$. A system of drift chambers (not shown)
 212 and two thin plastic scintillator counters T_0 and T_1 select decay e^+ 's emitted in the direction
 213 of \mathbf{B} . A 1-mm-thick magnetized Vacoflux 50TM foil (49% Fe, 49% Co, 2%V) in the central
 214 region with its polarized e^- ($P_{e^-} = 7.2\%$) serves as polarization analyzer. The two γ 's from e^+
 215 annihilation-in-flight with the polarized e^- are selected by an array of 91 interior $\text{Bi}_4\text{Ge}_3\text{O}_{12}$
 216 (BGO) crystals with plastic veto counters in front of them to reject charged particles. The

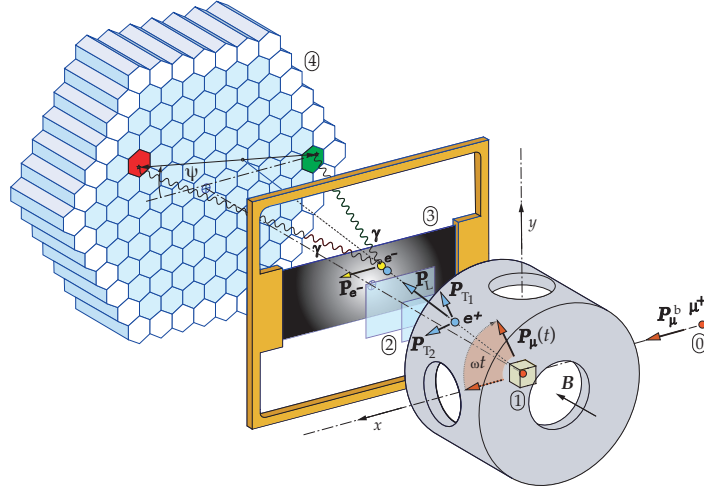


Figure 6.4: Schematic view of the experimental setup for the measurement of P_T . **0**: Burst of polarized muons (angular frequency ω , polarization \mathbf{P}_μ^b). **1**: Be stop target and precession field B . **2**: Two plastic scintillation counters selecting decay positrons **3**: Magnetized Vacoflux 50TM foil serving as a polarization analyzer. **4**: Array of 127 BGO scintillators to detect the two γ 's from e^+ annihilation-in-flight. From [23].

217 outer layer of 36 BGOs assists in an efficient collection of the deposited energy. Valid events
 218 are selected by using the correlation between the γ energies and their opening angle. The
 219 intensity distribution of the two γ 's has roughly the shape of the figure eight with a maximum
 220 in the direction of the bisector of $\mathbf{P}_T(t)$ and the e^- polarization \mathbf{P}_{e^-} [11, 24] (see Figure 6.3).
 221 The precession of $\mathbf{P}_\mu(t)$ implies a precession of $\mathbf{P}_T(t)$, while \mathbf{P}_{e^-} remains constant in time.
 222 Thus the intensity distribution of the γ 's also precesses with frequency ω . For any given pair
 223 ij of BGO detectors we ideally expect a signal for the normalized annihilation rate $N_{ij}(t)$ in
 224 the form

$$N_{ij}(t) = 1 + a_{ij} \cos(\omega t + \delta_0) + b_{ij} \sin(\omega t + \delta_0), \quad (6.45)$$

225 where t denotes the time the e^+ traverses counter T_0 and δ_0 an instrumental phase common
 226 to all time spectra. The events are contained in a time window of 39.5 ns total width, corre-
 227 sponding to two periods of the accelerator RF. The Fourier coefficients a_{ij} and b_{ij} contain the
 228 complete information of the transverse positron polarization. The analyzing power for anni-
 229 hilation in flight is large in most of the kinematic regions of the experiment. Figure 6.5 shows,
 230 as an example, the contour lines for the transverse analyzing power A_x (in %) as a function
 231 of the sum $u = (E_3 + E_4)/m_e$ and the difference $v = (E_3 - E_4)/m_e$ of the normalized photon
 232 energies E_3 and E_4 .

233 Due to the finite acceptance solid angle for events, the rate of ANN events also varies with
 234 the frequency ω because of a small muon spin rotation (μ SR) decay asymmetry modulated
 235 by the precessing $\mathbf{P}_\mu(t)$. By adding or subtracting the Fourier coefficients of appropriate pairs
 236 ij and $i'j'$, it was possible to derive either the μ SR - or the P_T signal, respectively. The μ SR
 237 signal is essential for the experiment, as it allows the decomposition of the vector \mathbf{P}_T into its
 238 components (P_{T_1}, P_{T_2}) , since \mathbf{P}_{T_1} lies in the plane of \mathbf{k}_{e^+} and $\mathbf{P}_\mu(t)$ and \mathbf{P}_{T_2} perpendicular to
 239 that plane (see Figure 6.1).

240 Table 6.1 shows the results of the general and of a restricted analysis [23]. The average
 241 polarization components $\langle P_{T_1} \rangle$ and $\langle P_{T_2} \rangle$ have been calculated from the values of η , η'' , and
 242 α'/A , β'/A , respectively. Based on the most general 4-fermion contact interaction ("general

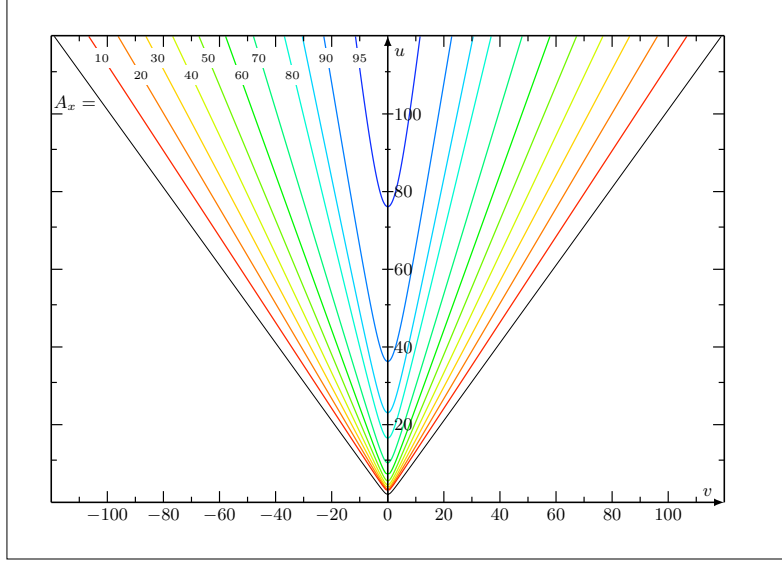


Figure 6.5: Contour lines for the transverse analyzing power A_x (in %) as a function of the sum $u = (E_3 + E_4)/m_e$ and the difference $v = (E_3 - E_4)/m_e$ of the normalized photon energies E_3 and E_4 . The outermost line is the kinematic boundary. From [11].

243 analysis") the parameter η is given by [12]

$$\eta = \frac{1}{2} \text{Re} \{ g_{LL}^V g_{RR}^{S*} + g_{RR}^V g_{LL}^{S*} + g_{LR}^V (g_{RL}^{S*} + 6g_{RL}^{T*}) + g_{RL}^V (g_{LR}^{S*} + 6g_{LR}^{T*}) \}. \quad (6.46)$$

244 With $g_{LL}^V \approx 1$, and all other $g_{\epsilon\mu}^\gamma \approx 0$ [7], one can simplify (6.46) considerably by neglecting all
 245 terms quadratic in non-standard couplings. This amounts to assuming one additional coupling
 246 beyond $V - A$. Then only two independent parameters remain ("restricted analysis"):

$$\eta = \frac{1}{2} \text{Re} \{ g_{RR}^S \}, \quad \beta'/A = -\frac{1}{4} \text{Im} \{ g_{RR}^S \}. \quad (6.47)$$

247 Here, g_{RR}^S is a scalar coupling with right-handed μ and e .

248 The Fermi coupling constant G_F is generally derived assuming an exclusive $V - A$ interac-
 249 tion, which amounts to setting $\eta = 0$. However, G_F depends on η [2, 12]:

$$G_F \approx G_F^{V-A} \cdot \left(1 - 2\eta \frac{m_e}{m_\mu} \right), \quad (6.48)$$

250 where m_e/m_μ is the mass ratio of electron and muon. Taking η into account increases the
 251 relative error $\Delta G_F/G_F$ from 9×10^{-6} to 360×10^{-6} (general analysis) resp. to 68×10^{-6}
 252 (restricted analysis).

253 Note that the results on α'/A , β'/A (and deduced from these, $\langle P_{T_2} \rangle$ and $\text{Im} \{ g_{RR}^S \}$) are the
 254 only experimental data sensitive to the violation of time reversal invariance (TRI) for a purely
 255 leptonic *reaction*. In contrast to the violation of TRI in the neutral kaon system [26], a T -
 256 odd observable in muon decay would be due to an interference between two couplings with
 257 different phase angles and thus be an unambiguous signal of new physics beyond the Standard
 258 Model.

	$V-A$	General analysis	Restricted analysis
η	0	$71 \pm 37 \pm 5$	$-2.1 \pm 7.0 \pm 1.0$
η''	0	$105 \pm 52 \pm 6$	$\equiv -\eta$
α'/A	0	$-3.4 \pm 21.3 \pm 4.9$	$\equiv 0$
β'/A	0	$-0.5 \pm 7.8 \pm 1.8$	$-1.3 \pm 3.5 \pm 0.6$
$\rho_{\eta\eta''}$		946	—
$\rho_{\alpha'\beta'}$		-893	—
$\chi^2/\text{d.o.f.}$		46.2/33	50.3/35
$\text{Re}\{g_{RR}^S\}$	0	—	$-4.2 \pm 14.0 \pm 2.0$
$\text{Im}\{g_{RR}^S\}$	0	—	$5.2 \pm 14.0 \pm 2.4$
$\langle P_{T_1} \rangle$	-3	$6.3 \pm 7.7 \pm 3.4$	
$\langle P_{T_2} \rangle$	0	$-3.7 \pm 7.7 \pm 3.4$	

Table 6.1: $V-A$ values and experimental results. All values, except $\chi^2/\text{d.o.f.}$, in units of 10^{-3} . The correlation coefficients ρ_{ij} are all compatible with zero except the two coefficients listed. The errors are statistical and systematic.

259 6.5.3 Electron Decay Asymmetry

260 The measurement of the electron decay asymmetry, $\mathcal{A}(x)$, from polarized muons [27], deter-
 261 mines how strongly the chiral components (L, R) of the muon take part in the interaction. This
 262 has been used to search for right-handed currents and other muon decay modes outside the
 263 Standard Model.

264 If the combination

$$\begin{aligned} \frac{1}{18}(9 + 3\xi - 16 \cdot \xi \cdot \delta) &= \frac{1}{4}|g_{RR}^S|^2 + \frac{1}{4}|g_{LR}^S|^2 + |g_{RR}^V|^2 + |g_{LR}^V|^2 + 3|g_{LR}^T|^2 \\ &\equiv Q_{RR} + Q_{LR} \equiv Q_R^\mu. \end{aligned} \quad (6.49)$$

265 has a value different from zero, then a coupling to the right-handed component of the muon
 266 has to exist, i.e. at least one $g_{eR}^\gamma \neq 0$. Conversely, if $Q_R^\mu = 0$, then the coupling acts exclusively
 267 on the left-handed muon.

268 The distribution of the flight direction of the positrons (electrons) is given by (6.5) with
 269 $\mathbf{P}_e = 0$ as

$$\frac{d^2\Gamma}{dx d\cos\vartheta} \equiv w(x, \vartheta) \sim \{F_{IS}(x) \pm P_\mu \cos\vartheta F_{AS}(x)\}. \quad (6.50)$$

270 This depends on the reduced energy, x , the angle ϑ between the muon polarization and the
 271 positron momentum as chosen by the detector, and on the degree of polarization $P_\mu > 0$. The
 272 asymmetry

$$\mathcal{A}(x) \equiv \frac{w(x, 0) - w(x, \pi)}{w(x, 0) + w(x, \pi)} = P_\mu \cdot \frac{F_{IS}(x)}{F_{AS}(x)} \quad (6.51)$$

273 depends on the parameters ϱ , η , ξ and $\xi\delta$ (see Eqs. (6.13a), (6.13b), (6.14a) and (6.14b)).

274 The distributions of the flight directions of the positrons (electrons) as seen by an apparatus

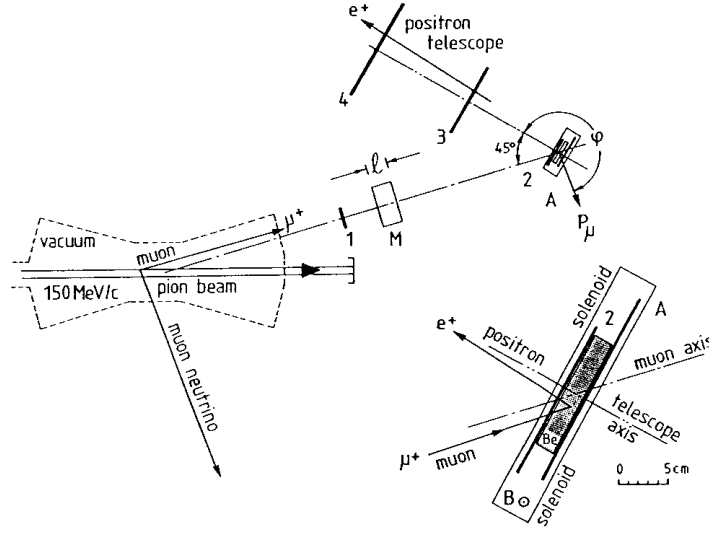


Figure 6.6: Muon Spin Rotation apparatus used to measure the integral asymmetry of the e^+ direction distribution following the decay of highly polarized muons. A parallel beam of monoenergetic (150 MeV/c) pions decays in flight in vacuum. Muons with energies within a well-determined interval are selected to stop in a beryllium plate, Be, employing a moderator of length ℓ . The original orientation of the muon polarization vector P_μ is thus defined. A rectangular solenoid produces a vertical magnetic field $B = 3$ mT causing the polarization of the stopped muons to precess in the horizontal plane. This gives rise to a sinusoidal modulation of the exponential decrease of the positron rate. The amplitude of the modulation ($\approx 1/3$) is proportional to the quantity desired, $P_\mu \xi$. From [27].

275 that is equally sensitive to positrons of all energies is given by

$$\begin{aligned} \frac{d\Gamma}{d \cos \vartheta} &\sim \int_{x_0}^1 dx \cdot \sqrt{x^2 - x_0^2} \cdot F_{IS}(x) \pm P_\mu \cos \vartheta \cdot \int_{x_0}^1 dx \cdot \sqrt{x^2 - x_0^2} \cdot F_{AS}(x) \\ &\sim (1 \pm \mathcal{A}' \cdot \cos \vartheta). \end{aligned} \quad (6.52)$$

276 The integral asymmetry, \mathcal{A}' , is proportional to $P_\mu \cdot \xi$ and depends on η in first order and on δ
277 in second order of x_0 . Neglecting x_0 ($x_0 = 0$) one obtains

$$\mathcal{A}' = \frac{1}{3} \cdot P_\mu \cdot \xi. \quad (6.53)$$

278 This allows the determination of ξ from an experiment using muons of known polarization.
279 In the analysis, the knowledge of the values of other muon decay parameters is unimportant.
280 Muon beams produced from pions decaying in flight in vacuum avoid Coulomb multiple
281 scattering. The muon spin lies in the plane of the laboratory line of flight of the original pion,
282 \mathbf{k}_π , and its decay muon, \mathbf{k}_μ . It points inwards (towards \mathbf{k}_π) for μ^+ and outwards for μ^-
283 (see Figure 6.6). The transverse and longitudinal muon spin components, ζ_T and ζ_L with
284 respect to the muon's laboratory line-of-flight are simply given by

$$\zeta_T = \frac{\sin \vartheta_\mu}{\sin \Theta_\mu}, \quad \zeta_L = \mp \sqrt{1 - \zeta_T^2}, \quad (6.54)$$

285 where the upper (lower) sign applies for the muon emitted with smaller (larger) momentum
 286 for the given angle of emission ϑ_μ , and where

$$\begin{aligned} \vartheta_\mu &= \text{laboratory angle between } \mathbf{k}_\pi \text{ and } \mathbf{k}_\mu, \\ \Theta_\mu &= \text{maximum laboratory angle by kinematics (Jacobian peak angle)}, \\ \sin \Theta_\mu &= (m_\pi^2 + m_\mu^2) / (2m_\pi k_\pi), \\ k_\pi &= \text{pion beam momentum.} \end{aligned}$$

287 The selection of a small slice of muon energy in the laboratory in the vicinity of the Jacobian
 288 peak corresponds to a choice of a small range of neutrino directions and thus of a degree of
 289 polarization $P_\mu = G \cdot P_{\nu_\mu}$. The geometrical factor G , which also has been studied experimentally
 290 [28], is close to one (> 0.99), and it is known with an uncertainty of $< 10^{-3}$ [27].

291 To measure the decay asymmetry, the muons are stopped in a metal (Be, Al) immersed in
 292 a transverse magnetic field where the spins precess. Detectors track the muon and the decay
 293 positron momenta. The positron intensity has a time modulation corresponding to the decay
 294 asymmetry. It is fortunate that there are substances (Al, Cu, Ag, Au, bromoform) that barely
 295 influence the spin direction of muons inside them. The disappearance of muon polarization
 296 during slowing down [21, 29] and thermalisation [30], i.e. at earlier times compared to the
 297 muon precession time, mimics a smaller \mathcal{A}_{exp} . Depolarization at later times is seen in the data
 298 [31, 32]. It can be accounted for by extrapolating the precession signal amplitude to time zero.
 299 The determination of the extrapolating-function parameters in the same experiment generally
 300 considerably reduces the statistical significance of the data due to their strong correlation with
 301 the signal. The relaxation time in pure metals at room temperature is often conveniently large
 302 compared to the muon lifetime.

303 Positron detectors with low energy thresholds are used for the measurement of $P_\mu \xi$. The
 304 result obtained from this experiment is [27]

$$P_\mu^\pi \xi = (1002.7 \pm 7.9_{\text{stat.}} \pm 3.0_{\text{syst.}}) \times 10^{-3}. \quad (6.55)$$

305 As ξ is not limited close to the measured value of $P_\mu \xi$, we cannot draw any specific conclusion
 306 on P_μ and ξ separately. In fact, $-3 \leq \xi \leq +3$. To isolate ξ from $P_\mu \xi$, one has to deduce P_μ
 307 from the measurement of $P_\mu \xi \delta / \rho$ of [32].

308 6.6 Results for τ -lepton and neutrino physics

309 For muon decay, we have shown that a hamiltonian with parity-odd and -even terms is not well
 310 suited for the description of a fully parity-violating interaction. Thus we have extended the
 311 concept of the *chiral* hamiltonian to leptonic τ decays [34]. Assuming universality for leptonic
 312 τ decays sensitivities for the different τ decay constants can be derived.

313 For the complete determination of the interaction in muon decay, it was essential to have
 314 experimental proof that the helicity of left-handed ν_μ is equal to -1 . Previous measurements
 315 had yielded $h_{\bar{\nu}_\mu} = (+990 \pm 160) \times 10^{-3}$ [35] and $h_{\nu_\mu} = (-1060 \pm 110) \times 10^{-3}$ [36]. It was then
 316 realized that the measurement of $P_\mu \xi \delta / \rho$ in muon decay by Carr et al. [37] not only yields
 317 a new lower limit for a possible right-handed W_R boson, but is also suited to derive a vastly
 318 improved limit for the helicity of the ν_μ [38]:

319 The normalized positron rate $d^2\Gamma/dx d \cos \vartheta$ at the spectrum end point can be written as

$$\frac{d^2\Gamma}{dx d \cos \vartheta} = (1 + P_\mu \cdot (\xi \delta / \rho) \cdot \cos \vartheta). \quad (6.56)$$

320 It is obvious that the factor $|P_\mu \xi \delta / \rho| \leq 1$, since the rate cannot be negative. P_μ is the polar-
 321 ization of the muon from the decay $\pi^+ \rightarrow \mu^+ \nu_\mu$ and independent of the muon decay constant.

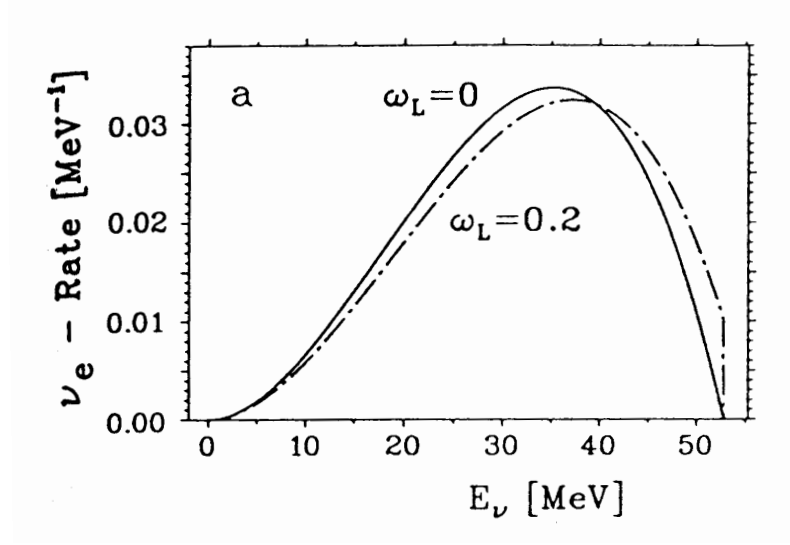


Figure 6.7: Normalized energy distributions of left-handed ν_e from the decay of unpolarized μ^+ . The spectrum shape parameter ω_L is the analog of the Michel parameter ρ of the e^+ . For a pure $V-A$ interaction ω_L is equal to zero. From [33].

322 Therefore we find

$$|P_\mu| \leq 1 \quad \text{and} \quad |\xi\delta/\rho| \leq 1. \quad (6.57)$$

323 On the other hand, from the measurement one gets a lower limit for the product [37]

$$P_\mu \xi \delta / \rho > 995.9 \times 10^{-3} \quad (90\% \text{CL}). \quad (6.58)$$

324 Since $P_\mu = -h_{\nu_\mu}$ we derive a lower limit for $|h_{\nu_\mu}|$ [38]:

$$|P_\mu| = |h_{\nu_\mu}| > 995.9 \times 10^{-3} \quad (90\% \text{CL}). \quad (6.59)$$

325 It has also been realized that experiments that detect the ν_e from the decay of unpolarized
 326 μ^+ by the reaction $^{12}\text{C}(\nu_e, e^-)^{12}\text{N}(\text{g.s.})$ not only determine the neutrino absorption cross sec-
 327 tion but also measure the ν_e energy spectrum [33]. The energy spectrum can be described by
 328 the spectrum shape parameters ω_L and η_L for left-handed and ω_R and η_R for right-handed
 329 ν_e . In contrast to the energy spectrum of the electrons it allows a new null-test of the standard
 330 model [33]. The right-handed ν_e cannot be detected as they are sterile in matter. For the
 331 energy spectrum of the left-handed ν_e one obtains

$$\frac{d\Gamma_L}{dy} = \frac{m_\mu^5 G_F^2}{16\pi^3} \cdot Q_L^{\nu_e} \cdot \{F_1(y) + \omega_L \cdot F_2(y) + \eta_L x_0 F_3(y)\}. \quad (6.60)$$

332 Here, $d\Gamma/dy$ is the probability of a left-handed ν_e to be emitted with the reduced energy
 333 $y = 2E_\nu/m_\mu$. The functions $F_1(y)$, $F_2(y)$ and $F_3(y)$ are given in [33]. The probability $Q_L^{\nu_e}$ of
 334 the ν_e to be left-handed, the spectral shape parameter ω_L and the low energy parameter η_L

335 are

$$Q_L^{\nu_e} = \frac{1}{4}|g_{RL}^S|^2 + \frac{1}{4}|g_{RR}^S|^2 + |g_{LL}^V|^2 + |g_{LR}^V|^2 + 3|g_{RL}^T|^2 = \frac{1}{2}(1 - P_{\nu_e}), \quad (6.61)$$

$$\omega_L = \frac{3}{4} \frac{\{|g_{RR}^S|^2 + 4|g_{LR}^V|^2 + |g_{RL}^S + 2g_{RL}^T|^2\}}{\{|g_{RL}^S|^2 + |g_{RR}^S|^2 + 4|g_{LL}^V|^2 + 4|g_{LR}^V|^2 + 12|g_{RL}^T|^2\}}, \quad (6.62)$$

$$\eta_L = 2 \frac{\text{Re}\{g_{LL}^V g_{RR}^{S*} + g_{LR}^V (g_{RL}^{S*} + 6g_{RL}^{T*})\}}{\{|g_{RL}^S|^2 + |g_{RR}^S|^2 + 4|g_{LL}^V|^2 + 4|g_{LR}^V|^2 + 12|g_{RL}^T|^2\}}, \quad (6.63)$$

336 where P_{ν_e} denotes the longitudinal polarization of the ν_e . Figure 6.7, as an example, shows
 337 the normalized energy distributions for the $V - A$ prediction $\omega_L^{V-A} = 0$ and for $\omega_L = 0.2$. A
 338 value $\omega_L > 0$ results in events at the spectrum end where none are expected for the $V - A$
 339 interaction.

340 References

- 341 [1] L. Michel, *Interaction between four half spin particles and the decay of the μ meson*, Proc.
 342 Phys. Soc. **A63**, 514 (1950).
- 343 [2] F. Scheck, *Muon physics*, Phys. Rept. **44**, 187 (1978).
- 344 [3] T. Kinoshita and A. Sirlin, *Polarization of electrons in muon decay with general parity*
 345 *nonconserving interactions*, Phys. Rev. **108**, 844 (1957).
- 346 [4] M. Fierz, Z. Physik **101**, 553 (1937).
- 347 [5] F. Scheck, *Leptons, Hadrons and Nuclei*, North-Holland, Amsterdam (1983).
- 348 [6] K. Mursula and F. Scheck, *Analysis of leptonic charged weak interactions*, Nucl. Phys.
 349 **B253**, 189 (1985).
- 350 [7] W. Fetscher, H. J. Gerber and K. F. Johnson, *Muon decay: Complete determination of the*
 351 *interaction and comparison with the standard model*, Phys. Lett. **B173**, 102 (1986).
- 352 [8] F. Scheck, *Electroweak and strong interactions: An introduction to theoretical particle*
 353 *physics*, Springer, Berlin (1996).
- 354 [9] C. Bouchiat and L. Michel, *Theory of μ -meson decay with the hypothesis of nonconserving*
 355 *of parity*, Phys. Rev. **106**, 170 (1957).
- 356 [10] T. Kinoshita and A. Sirlin, *Muon decay with parity nonconserving interactions and radiative*
 357 *corrections in the two-component theory*, Phys. Rev. **107**, 593 (1957).
- 358 [11] W. Fetscher, *Annihilation-in-flight of polarised positrons with polarised electrons as an*
 359 *analyser of the positron polarisation from muon decay*, Eur. Phys. J. C **52**, 1 (2007),
 360 doi:10.1140/epjc/s10052-007-0384-6.
- 361 [12] W. Fetscher and H. J. Gerber, in *Precision Tests of the Standard Electroweak Model*,
 362 chap. *Precision Tests in Muon and Tau Decays*, pp. 657–705, ed. P. Langacker, World
 363 Scientific, Singapore (1995).
- 364 [13] H. Burkard et al., *Muon decay: Measurement of the transverse positron polarization and*
 365 *general analysis*, Phys. Lett. **B160**, 343 (1985).

- 366 [14] H. Burkard *et al.*, *Muon decay: Measurement of the positron polarization and implications*
367 *for the spectrum shape parameter eta, v-a and t invariance*, Phys. Lett. **B150**, 242 (1985).
- 368 [15] H.-J. Gerber, *Lepton properties*, International Europhysics Conference on High Energy
369 Physics (1987).
- 370 [16] C. Jarlskog, Nucl. Phys. **75**, 659 (1966).
- 371 [17] S. Mishra *et al.*, *Inverse Muon Decay, $\nu_{\mu}e \rightarrow \mu^{-}\nu_e$, at the Fermilab Tevatron*, Phys. Lett. B
372 **252**, 170 (1990), doi:[10.1016/0370-2693\(90\)91099-W](https://doi.org/10.1016/0370-2693(90)91099-W).
- 373 [18] D. Geiregat *et al.*, *A New measurement of the cross-section of the inverse muon decay*
374 *reaction muon-neutrino $e^{-} \rightarrow \mu^{-}$ electron-neutrino*, Phys. Lett. B **247**, 131 (1990),
375 doi:[10.1016/0370-2693\(90\)91061-F](https://doi.org/10.1016/0370-2693(90)91061-F).
- 376 [19] H. Toelhoek, Rev. Mod. Phys. **28**, 277 (1956).
- 377 [20] J. DeRaad, Lester L. and Y. J. Ng, *Electron Electron Scattering. 3. Helicity*
378 *Cross-Sections for electron Electron Scattering*, Phys. Rev. D **11**, 1586 (1975),
379 doi:[10.1103/PhysRevD.11.1586](https://doi.org/10.1103/PhysRevD.11.1586).
- 380 [21] G. Ford and C. Mullin, *Scattering of Polarized Dirac Particles on Electrons*, Phys. Rev. **108**,
381 477 (1957), doi:[10.1103/PhysRev.108.477](https://doi.org/10.1103/PhysRev.108.477).
- 382 [22] R. Prieels *et al.*, *Measurement of the parameter ξ'' in polarized muon decay and implications*
383 *on exotic couplings of the leptonic weak interaction*, Phys. Rev. D **90**(11), 112003 (2014),
384 doi:[10.1103/PhysRevD.90.112003](https://doi.org/10.1103/PhysRevD.90.112003), [1408.1472](https://arxiv.org/abs/1408.1472).
- 385 [23] N. Danneberg *et al.*, *Muon decay: Measurement of the transverse polarization of the decay*
386 *positrons and its implications for the Fermi coupling constant and time reversal invariance*,
387 Phys. Rev. Lett. **94**, 021802 (2005), doi:[10.1103/PhysRevLett.94.021802](https://doi.org/10.1103/PhysRevLett.94.021802).
- 388 [24] F. Corriveau *et al.*, *Does the positron from muon decay have transverse polarization?*, Phys.
389 Lett. **B129**, 260 (1983).
- 390 [25] I. C. Barnett *et al.*, *An apparatus for the measurement of the transverse polarization of*
391 *positrons from the decay of polarized muons*, Nucl. Instrum. Meth. **A455**, 329 (2000).
- 392 [26] A. Angelopoulos *et al.*, *First direct observation of time-reversal non-invariance in the neu-*
393 *tral kaon system*, Phys. Lett. **B444**, 43 (1998).
- 394 [27] I. Beltrami, H. Burkard, R. Von Dincklage, W. Fetscher, H. Gerber, K. Johnson, E. Pe-
395 droni, M. Salzmann and F. Scheck, *Muon Decay: Measurement of the Integral Asymmetry*
396 *Parameter*, Phys. Lett. B **194**, 326 (1987), doi:[10.1016/0370-2693\(87\)90552-1](https://doi.org/10.1016/0370-2693(87)90552-1).
- 397 [28] I. Beltrami *et al.*, *Measurement of the integral asymmetry in mu decay and implication for*
398 *the wino mass*, Helv. Phys. Acta **60**, 611 (1987).
- 399 [29] J. Heintze, Z. Physik p. 560 (1957).
- 400 [30] F. G. J.H. Brewer, K.M. Crowe and A. Schenck, *Muon Physics*, vol. III, Academic, New
401 York (1975).
- 402 [31] D. Stoker *et al.*, *Search for Right-handed Currents Using Muon Spin Rotation*, Phys. Rev.
403 Lett. **54**, 1887 (1985), doi:[10.1103/PhysRevLett.54.1887](https://doi.org/10.1103/PhysRevLett.54.1887).

- 404 [32] A. Jodidio *et al.*, *Search for Right-Handed Currents in Muon Decay*, Phys. Rev. D **34**, 1967
405 (1986), doi:[10.1103/PhysRevD.34.1967](https://doi.org/10.1103/PhysRevD.34.1967), [Erratum: Phys.Rev.D 37, 237 (1988)].
- 406 [33] W. Fetscher, *Muon decay: Measurement of the energy spectrum of the electron-neutrino*
407 *as a novel precision test for the Standard Model*, Phys. Rev. Lett. **69**, 2758 (1992),
408 doi:[10.1103/PhysRevLett.69.2758](https://doi.org/10.1103/PhysRevLett.69.2758), [Erratum: Phys.Rev.Lett. 71, 2511 (1993)].
- 409 [34] W. Fetscher, *Leptonic tau decays: How to determine the Lorentz structure of the*
410 *charged leptonic weak interaction by experiment*, Phys. Rev. D **42**, 1544 (1990),
411 doi:[10.1103/PhysRevD.42.1544](https://doi.org/10.1103/PhysRevD.42.1544).
- 412 [35] R. Abela, G. Backenstoss, W. Kunold, L. Simons and R. Metzner, *Measurements of the*
413 *polarization of the 2P and 1S states in muonic atoms and the helicity of the muon in pion*
414 *decay*, Nucl. Phys. A **395**, 413 (1983), doi:[10.1016/0375-9474\(83\)90051-9](https://doi.org/10.1016/0375-9474(83)90051-9).
- 415 [36] L. Roesch, V. Telegdi, P. Truttmann, A. Zehnder, L. Grenacs and L. Palfy, *Measurement of*
416 *the average and longitudinal recoil polarizations in the reaction C-12 (μ^- , neutrino) B-12*
417 *(G.S.): pseudoscalar coupling and neutrino helicity*, Helv. Phys. Acta **55**, 74 (1982).
- 418 [37] J. Carr *et al.*, *Search for Right-Handed Currents in Muon Decay*, Phys. Rev. Lett. **51**, 627
419 (1983), doi:[10.1103/PhysRevLett.51.627](https://doi.org/10.1103/PhysRevLett.51.627), [Erratum: Phys.Rev.Lett. 51, 1222 (1983)].
- 420 [38] W. Fetscher, *Helicity of the muon-neutrino in π^+ decay: a comment on the measurement of*
421 *P (MU) XI DELTA / RHO in muon decay*, Phys. Lett. B **140**, 117 (1984), doi:[10.1016/0370-](https://doi.org/10.1016/0370-2693(84)91059-1)
422 [2693\(84\)91059-1](https://doi.org/10.1016/0370-2693(84)91059-1).